Plant Soil
DOI 10.1007/s11104-017-3333-7

REGULAR ARTICLE

Root volume distribution of maturing perennial grasses revealed by correcting for minirhizotron surface effects

Christopher K. Black · Michael D. Masters · David S. LeBauer · Kristina J. Anderson-Teixeira · Evan H. DeLucia

Received: 22 February 2017 / Accepted: 3 July 2017

Abstract
Aims Root architecture drives plant ecology and physiology, but current detection methods limit understanding of root placement within soil profiles. We developed a statistical model of root volume along depth gradients and used it to infer carbon storage potential of land-use changes from conventional agriculture to perennial bioenergy grasses.
Methods We estimated root volume of maize-soybean rotation and three perennial grass systems (*Miscanthus* × *giganteus*, *Panicum virgatum*, tallgrass prairie mix) by Bayesian modeling from minirhizotron images, correcting for small images and near-surface underdetection. We monitored seasonal and inter-annual changes in root volume distribution, then validated our estimates against root mass from core samples.
Results The model explained 29% of root volume variation and validated well against core mass. Seventh-year perennials had greater belowground biomass than maize-soybean both in total (11-16×) and throughout the profile (2-17× at every depth < 120 cm). Perennials' relative depth allocations were stable over time, while total root volume increased through five years. In 2012 a historically hot, dry summer damaged maize while perennials appeared resilient, suggesting their large-deep root systems aid drought resistance.
Conclusions Perennial root systems are large, deep, and persistent. Converting row crops to perennial bioenergy

Responsible Editor: Richard J. Simpson.

Electronic supplementary material The online version of this article (doi:10.1007/s11104-017-3333-7) contains supplementary material, which is available to authorized users.

C. K. Black · E. H. DeLucia (✉)
Department of Plant Biology, University of Illinois at Urbana-Champaign, 265 Morrill Hall, 505 South Goodwin Ave, Urbana, IL 61801, USA
e-mail: delucia@illinois.edu

C. K. Black · M. D. Masters · D. S. LeBauer · K. J. Anderson-Teixeira · E. H. DeLucia
Carl. R. Woese Institute for Genomic Biology, University of Illinois at Urbana-Champaign, Urbana, IL, USA

M. D. Masters · E. H. DeLucia
Institute for Sustainability, Energy, and Environment, University of Illinois at Urbana-Champaign, Urbana, IL, USA

K. J. Anderson-Teixeira
Conservation Ecology Center, Smithsonian Conservation Biology Institute, Front Royal, VA, USA

K. J. Anderson-Teixeira
Center for Tropical Forest Science – Forest Global Earth Observatory, Smithsonian Tropical Research Institute, Panama, Republic of Panama

Published online: 27 July 2017

grasses likely sequesters carbon in a large, potentially very stable, soil pool.

Keywords Minirhizotron · Stan · Bayesian modeling · Root volume · Root allocation

Introduction

The placement of plant roots in the soil profile is an ecological trait that affects many ecosystem properties. Deeper roots have high construction costs but provide structural support, give access to deep water and nutrient pools (Wasson et al. 2012; Zwicke et al. 2015), and store carbon (De Deyn et al. 2008). Meanwhile shallower roots are less costly to build, give access to larger but potentially less reliable water and nutrient pools (Lynch and Brown 2001; Hodge 2004; Nippert et al. 2012), and in multispecies systems shallow roots promote competitive success through root-zone exclusion (Genney et al. 2002). The existence of mycorrhizal associations lead to further tradeoffs between root architectures optimized for soil exploration by the root itself or by the mycorrhizal symbiont (Comas and Eissenstat 2009; Liu et al. 2015). Understanding root distributions is therefore fundamental to predicting ecosystem functioning (Bardgett et al. 2014) and improving management outcomes (Kochian 2016).

Quantifying root distribution is especially important in the context of understanding how land use affects soil C cycling. For instance, changes in land use from annual row-crop agriculture to perennial grasses managed for bioenergy production may build soil C, because bioenergy grasses have large root systems and minimal tillage requirements (Anderson-Teixeira et al. 2013; McCalmont et al. 2015; Agostini et al. 2015), and these C gains from bioenergy grasses may be especially persistent because of preferential allocation to deep soil and consequent slower turnover (Balesdent and Balabane 1996; Rasse et al. 2005; Kell 2011; Rumpel and Kögel-Knabner 2011; Agostini et al. 2015; Prieto et al. 2016; Ward et al. 2016). However, to evaluate this claim we need a better understanding of how much C is added, where it is distributed in the soil, and its turnover time (Agostini et al. 2015).

We know less about root dynamics such as depth distribution and turnover than we do about aboveground plant traits. This lack of detail is exacerbated by inherent limitations of the available methods for quantifying root systems (Pierret et al. 2005; Milchunas 2009; Topp et al. 2016). Container studies are subject to pot effects and therefore only realistic for very small plants (Poorter et al. 2012). Destructive harvesting approaches such as coring and trenching give accurate snapshots, but require massive effort (hours to days per sample; Bohm et al. 1977) and cannot be repeated through time. Furthermore, because the effort required for coring and trenching increases rapidly with depth, many such surveys have focused only on the shallow soil layers (typically 30 cm or less), often leading to severe underestimates of deep root mass (Mokany et al. 2006). Nondestructive imaging systems such as minirhizotrons give time-resolved data, but with the tradeoff that the data are noisier and indirect; the raw data are two-dimensional images that must be converted to a three-dimensional volume estimate and then converted again from a volume to a mass, with further possible noise and biases in the conversion (Metcalfe et al. 2007; Taylor et al. 2014).

Minirhizotron observations of standing root mass seem to be especially susceptible to depth biases. Previous research has found that minirhizotrons underdetect roots in the shallowest soil layers, probably because of poor contact between tube and soil in the least compacted and most frequently disturbed surface horizons (Bragg et al. 1983; Taylor et al. 1990; Parker et al. 1991; Samson and Sinclair 1994; Ephrath et al. 1999). Studies that considered this bias have typically avoided it by excluding data from the affected layers (potentially containing the majority of the root system; Samson and Sinclair 1994), by using paired comparisons within layers, or equivalently by developing depth-specific calibration factors. Furthermore, many minirhizotron studies only measure root length and calculate volume using a homogeneous diameter assumption, which further underestimates root volume (Rose 2017). These approaches are unsatisfactory for studies that seek to compare both total root volume and the fraction of roots found in each layer over time and among species.

In this study, we tracked the change in root volume associated with a change in management from annually tilled conventional row crops (maize and soybean) to untilled perennial grasses mowed annually for bioenergy feedstock. We used minirhizotrons to track seasonal and interannual patterns in root distribution to a depth of >1 m, developed a statistical model to account for biases from near-surface under detection and small samples, and verified our estimates with deep-soil core samples. We predicted that root volume under perennial grasses would be greater than under row crops, that root

systems would reach their maximum extents in the same year each crop achieved maturity as measured by aboveground yields, and that after statistical correction the root volumes obtained from minirhizotron images would show the same depth distribution as root masses obtained by coring.

Materials and methods

Site

Measurements were made at the University of Illinois Energy Farm, ~5 km south of Urbana, Illinois (40.06 N, 88.19 W, elevation 220 m). Climate, soils, and site establishment have been described in detail elsewhere (Zeri et al. 2011; Smith et al. 2013; Masters et al. 2016). Briefly, the site has a highly seasonal continental climate with a mean annual temperature of 11 °C (below 0 °C December–February, over 20 °C June–August) and average annual precipitation of approximately 1 m, with approximately half falling as rain during the growing season (May–September). Soils are deep and loess-derived, mapped as Argiudolls of the Dana, Flanagan, and Blackberry series of silt loams. Four cropping treatments, each representative of a possible bioenergy cropping scheme, were established in 2008: A three-year maize-maize-soybean rotation, a prairie restoration mix of 28 native species (Zeri et al. 2011), and two perennial grasses: *Miscanthus* × *giganteus* Greef and Deuter ex Hodkinson and Renvoize (*Miscanthus*; cv "Illinois") and *Panicum virgatum* L. (Switchgrass; cv "Cave-in-Rock"). The site was planted in a randomized complete block design replicated five times, with four blocks of 0.7 ha plots and one block of 3.8 ha plots (Masters et al. 2016). Each large plot was instrumented to record weather, crop growth parameters, and ecosystem C and water exchange.

Maize and soybeans were planted and harvested according to typical Central Illinois cropping practices, with tillage prior to maize plantings only. Switchgrass and prairie were planted in 2008 and not subsequently replanted; *Miscanthus* survived the first winter poorly and therefore the small *Miscanthus* plots were replanted in 2009 and the large *Miscanthus* plot was replanted in 2010. Standing biomass from perennials was mowed and baled after senescence each winter.

Maize was fertilized each year before planting (168–202 kg N ha^{-1} yr^{-1}); no fertilizer was applied to soybean. Switchgrass was fertilized with 56 kg N ha^{-1} yr^{-1} applied before crop emergence. Initially, neither prairie nor *Miscanthus* were fertilized. In 2014 the small *Miscanthus* plots were split and one half of each 0.7 ha plot remained unfertilized while the other half, and the entire large (3.8 ha) plot, received 56 kg N ha^{-1}. Because tube placement was determined before the N treatment was imposed, each split plot contained only two minirhizotron tubes and was therefore too sparsely sampled for reliable root volume estimates, so we did not attempt to estimate the effects of N treatment on *Miscanthus* root volume. Instead, we report all 2014 *Miscanthus* observations as means averaging across fertilizer treatments.

Rhizotron tube installation and maintenance

To observe root systems over time, in May of 2009 we installed 96 clear acrylic minirhizotron tubes. We placed 24 tubes in each crop, with 4 tubes (one in each quadrant) per 0.7 ha plot and 8 tubes (2 in each quadrant) per 3.8 ha plot. Each tube was 1.8 m L × 51 mm ID × 57 mm OD (Bartz Technology corporation, Carpinteria CA USA) and was installed using a tractor-mounted hydraulic probe (Giddings Machine Co., Windsor CO USA) at an angle 30° from vertical (Bragg et al. 1983). For perennial crops, we placed tubes randomly within each quadrant. For maize and soybean, we placed half the tubes in each plot directly within rows and the other half midway between rows. Each tube's vertical angle was aligned along a row, so comparisons of root density between depths in a single tube were not confounded with row placement. Each tube was inserted until 22 cm remained aboveground or until it was stopped by soil resistance, allowing image collection from the soil surface to a depth between 115 and 140 cm. The aboveground portion of each tube was capped to minimize intrusion of light, water, or temperature swings.

Tubes in maize and soybean plots were installed immediately after planting every spring and removed after harvest to allow tillage. The tubes in perennial crops remained permanently installed, but each winter a portion of the permanent tubes developed leaks in their bottom end caps, and were replaced the following spring in a freshly bored hole at least 1 m away from the previous location. Of the original 72 tubes 'permanently' installed at the site in 2009, 39 survived to the end of the experiment in their initial location. Because of ongoing tube failures after repeated installation and a

limited stock of replacement tubes, in 2014 we were only able to collect images from 8 tubes in maize, all in the 3.8 ha block. Tubes in perennial crops were less affected by these failures and at least 20 tubes in each perennial crop remained usable in 2014.

Image collection

From 2010 through 2013 we collected images approximately once a month during the growing season (May to October), and in 2014 we collected images once in August, at peak aboveground biomass. Prior to each measurement we used a long-handled swab to clean dust and condensation off the inner surface of the tube. We then mounted a portable minirhizotron camera (BTC-100×; Bartz Technology) into the tube and collected images at ~6-cm vertical increments until the camera reached the bottom of the tube (typically ~125 cm). Each tube's offset from the soil surface was remeasured periodically and used to correct image depth estimates. The 6-cm vertical increment came from collecting images every five stops of the depth-indexing handle (13.5 mm per stop = (5 • 1.35) • cos(30°) = 5.8 cm) and was chosen as the spacing that best balanced adequate sampling from each tube against the time required to process each image after collection (Johnson et al. 2001).

The resulting images were 754 × 510 pixels and the camera was calibrated daily by photographing a 1 × 1 mm grid attached to the outside of a short length of rhizotron tube (same viewing distance as the roots). The final maximum image resolution was ~0.025 mm per pixel.

Image processing

In the laboratory, we recorded the length and diameter of every visible root segment by manual tracing using WinRHIZO TRON MF v. 2009a (Regent Instruments, Québec QC, Canada) and performed all downstream analyses on the total volume of root visible in each image assuming each root segment was a perfect conic section with dimensions ($Diameter_{start}$ × $Diameter_{end}$ × length). Rhizotron methods have low success distinguishing living from dead root tissue (Iversen et al. 2011), so we made no attempt to classify tissue death status. Thus, all root density estimates include visible root necromass.

To minimize human variation in root tracing, all technicians were trained using the same set of representative images and the agreement in traced root volume from each image was taken as an estimate of the variation among workers given the same task. The variation among workers was less than the within-worker variation (95% intervals: sd among workers = 1.2–1.6 mm^3 img^{-1}, sd within worker = 2.4–2.7 mm^3 img^{-1}; data not shown), indicating that technician identity was a minor contributor to the variation in the tracing step. Since these agreement scores were taken from novice tracers immediately after the completion of their training, it is likely that they somewhat overstate the actual variation from experienced technicians.

After tracing, each season's data were aggregated using a set of custom R scripts to adjust observed root volumes for differences in image magnification, remove data from images with poor image quality, convert locations within each tube to depths below the soil surface, and aggregate results across experimental blocks.

Root mass measurements

To compare estimates of root density from minirhizotrons and destructive coring methods, we collected deep-soil cores. In August of 2011 and of 2014, when aboveground biomass of all four crops was near its yearly maximum, we collected soil cores to a depth ≥ 100 cm from 24 locations within each crop (4 from each 0.7 ha plot, 8 from each 3.8 ha plot) using a tractor-mounted hydraulic corer (Giddings Machine Co.). Because the heavy coring equipment necessitated trampling a large (2–3 × 2–3 m) quadrat at every location, coring locations were all within 5 m of a plot edge. At each location, three 3.8 cm diameter cores were collected from within a 1-m area. We divided each core into five depth horizons (0–10, 10–30, 30–50, 50–100, and 100+ cm), pooled horizons from the same location, then separated root and rhizome material from soil by hydropneumatic elutriation (Roberts et al. 1993), separated rhizomes from roots by hand-sorting, oven-dried both to constant mass, and weighed them.

Since individual locations within a plot are pseudoreplicates, we calculated block means of root mass per cm^3 soil (for depth-resolved analyses) or per

m^2 ground area (for whole-profile totals), log-transformed the result, then fitted a mixed-effects linear model where ln(depth) is a continuous covariate, crop and year are categorical fixed effects (Eq. 1), block is a categorical random effect (Eq. 2), and residuals follow a first-order autoregressive function within each level of the (block by crop by year) interaction to account for the autocorrelation between adjacent depths (Eq. 3).

$$\ln\left(y_{ijk\ell}\right) = \beta_i \mathrm{crop}_i + \beta_j \mathrm{year}_j + \beta_k \ln(\mathrm{depth}_k) + \gamma_\ell \mathrm{block}_\ell + \epsilon_{ijk\ell} \quad (1)$$

$$\gamma_\ell \sim N\left(0, \psi^2_{ijk}\right) \quad (2)$$

$$\epsilon_{ijk\ell} \sim N\left(0, \sigma^2 \lambda_{ijk\ell}\right), \mathrm{corr}\left(\epsilon_{ijkl}, \epsilon_{ijk\ell'}\right) \sim \phi^{|\ell' - \ell|} \quad (3)$$

All root core statistics were performed in R version 3.3.2 (R Core Team 2016) using nlme 3.1 (Pinheiro et al. 2016) for linear model fits followed by lsmeans 2.25 (Lenth 2016) for predicted marginal means and post-hoc treatment comparisons, using Tukey's method to adjust for multiple comparisons. The data from 2011 have been presented previously (Anderson-Teixeira et al. 2013); we limit our discussion here to the comparison against simultaneously collected rhizotron images from the same plots.

Bayesian modeling of root volume

To estimate root volume from the root areas traced from minirhizotron images, we used a Bayesian model to integrate image data with prior knowledge about plant architecture and growth patterns to produce a mathematically tractable and physiologically defensible estimate of root volume density and depth distribution in each crop. The basic structure of the model is a log-linear mixed model much like Eq. 1, with the addition of a zero-inflation term previously formulated for root production estimates and a novel empirical correction for the minirhizotron surface effect.

To construct the model, we began with a log-linear mixed model of root volume (mm^3 root observed per mm^2 of image traced) similar to the one used for root mass from cores (Eq. 1). On a given sampling day, the expected log root density μ_{ijk} (Eq. 4) declines with log depth according to a crop-specific intercept α_i and slope β_i, and the intercept varies for each sampling location (i.e. minirhizotron tube) as a zero-centered random effect $\gamma_j \sim N(0, \sigma^{\mathrm{tube}})$:

$$\mu_{ijk} = \alpha_i + \gamma_j + \beta_i \ln(\mathrm{depth}_k) \quad (4)$$

We treated individual minirhizotron tubes as the unit of replication (rather than block means as in the core data) because the observed variation among individual minirhizotron tubes was much larger than the variation among blocks and therefore subsumes the block effects. It should be possible to calculate the block effect, if it is needed, as the mean of the estimated tube effect coefficients of all tubes in that block.

Next, we added an empirical correction for reduced minirhizotron root detection efficiency near the soil surface. The cause of this underdetection is still unclear, but it is commonly observed in minirhizotron studies (Bragg et al. 1983; Taylor et al. 1990; Samson and Sinclair 1994; Ephrath et al. 1999; Gray et al. 2016). We corrected for this underdetection by noting that when measured directly it appears to be sigmoid with depth (Fig. S1), and when not measured it can be inferred by a visible deviation from the log-linear depth trend in near-surface layers, meaning the correction can be found by solving for a sigmoid underdetection function that brings near-surface observations back toward the linear depth model of Eq. 4. Then the expected density of *detected* roots $\hat{\mu}$ (Eq. 5) is

$$\hat{\mu}_{ijk} = \frac{\mu_{ijk}}{1 + \exp\left(-\left(\alpha_i^{\mathrm{surface}} + \beta_i^{\mathrm{surface}} \mathrm{depth}_k\right)\right)} \quad (5)$$

where $\alpha_i^{surface}$ is the depth where the surface underdetection effect reduces observed root volume to 50% of true root volume, $\beta_i^{surface}$ scales the rate of increase in root detection with depth, and both are estimated from observations but informed by prior research (Sec. S1) via Bayesian priors that are "weakly informative" in the sense of Gelman (2006).

Finally, we accounted for small sample size effects by incorporating the zero-inflation term presented by Sonderegger et al. (2013), specifically their Eqs. 1 & 2. This correction is motivated by noting that individual images are small (~240 mm^2) compared to the scale of root system heterogeneity, and many images contain no visible roots even when root density is high. The

observed root volume in an individual image (Eq. 6) therefore follows a mixture distribution

$$y_{ijk} \sim \begin{cases} \log N\left(\hat{\mu}_{ijk}, \sigma^2\right), \text{with probability } \phi_{ijk} \\ 0, \text{with probability } 1-\phi_{ijk} \end{cases} \quad (6)$$

where the probability ϕ_{ijk} of observing any roots (Eq. 7) increases with expected root density $\hat{\mu}_{ijk}$ (Eq. 5) as

$$\ln \frac{\phi_{ijk}}{1-\phi_{ijk}} = \alpha^{\text{detect}} + \beta^{\text{detect}} \hat{\mu}_{ijk} \quad (7)$$

We fitted this model separately to each day of data using the Rstan (Stan Development Team 2016a) interface to the Stan probabilistic programming language (Stan Development Team 2016b; Carpenter et al. 2017), which computes the joint likelihood of all model parameters given the observed data and uses Hamiltonian Monte Carlo sampling to draw from their posterior distributions. For each model, we ran five independent chains for 5000 iterations each, then discarded the first 1000 iterations as burn-in, giving a total of 20,000 Monte Carlo samples for each parameter and an effective posterior sample size (after accounting for autocorrelation) of at least 1000. We checked for convergence both visually by plotting the chains and by checking that the potential scale reduction factor was less than 1.05 (Gelman and Rubin 1992). Prior distributions for each parameter are shown in Fig. S2 and their values are justified in Sec. S1. All data and scripts from the analysis are available online (https://github.com/infotroph/efrhizo) and have been deposited in the Dryad digital repository (Black et al. 2017).

Results

Soil core samples

Perennials produced far more root biomass than maize, and the difference became larger as the perennials matured (Fig. 1). The root biomass of the perennial grasses in core samples increased dramatically from 2011 to 2014 ($F_{1,28} > 66$; $p < 0.01$), from 5 to 8 times greater than maize in 2011 (Anderson-Teixeira et al. 2013) to 8–11 times greater than maize in 2014 (Fig. 1; all Tukey comparisons between maize and individual perennials yield $t_{28} > 7$; all $p < 0.01$). Root biomass increased in *Miscanthus* and prairie from 2001 to 2014 (both more than tripled; all Tukey $t_{28} > 5.5$, $p < 0.01$) but not in

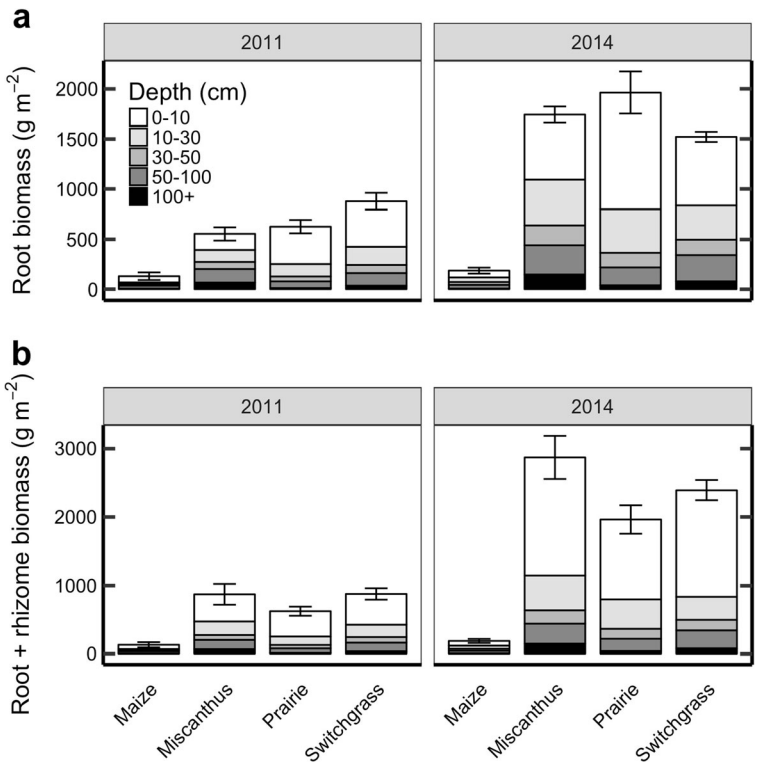

Fig. 1 Biomass in roots and rhizomes of bioenergy crops, as measured by coring in 2011 and again in 2014, divided by depth horizon. Error bars show mean ± 1 standard error of total profile biomass in each block. The 2011 data are re-plotted from (Anderson-Teixeira et al. 2013)

maize or switchgrass (root mass was greater by 62% and 76% respectively, but the difference was not significant; Tukey $t_{28} < 2.8$; $p > 0.15$). When including the mass of rhizomes as well as roots, the total (root + rhizome) belowground biomass of perennials increased to 11–16 times that of maize in 2014 and the year-over-year changes were similar in magnitude to those for roots alone, but the variability was greater and the year by crop interaction was not significant ($F_{3,28} = 2.2$; $p > 0.1$).

There were no statistically resolvable differences in total belowground biomass among perennials in either year (all Tukey $t_{28} < 1.6$; $p > 0.4$), but the rank order of total mass depended on the year and the pool measured because of increases in rhizome mass. In 2011 switchgrass had the greatest mass (860 ± 126 g root m^{-2}, no rhizomes detected) and *Miscanthus* was second for total biomass (819 ± 130 g root + rhizome m^{-2}) but third for roots alone (535 ± 79 g root m^{-2}). In 2014 prairie had the greatest root mass (1924 ± 282 g root m^{-2}) but *Miscanthus* had the greatest total mass (2793 ± 444 g root m^{-2}). For comparison, maize root mass was 109 ± 17 (2011) and 177 ± 26 (2014) g root m^{-2} (Fig. 1).

Biomass in core samples declined approximately log-linearly with depth (Fig. 2), but the distribution of biomass through the soil profile varied by cropping system ($F_{3,180} = 8.69$, $p < 0.01$). Prairie roots were more concentrated near the surface and declined more quickly with depth than *Miscanthus* or maize (both $t_{180} > 3.5$; $p < 0.01$). The decline in switchgrass was intermediate between prairie and maize and not significantly different from either one (both $t_{180} < 2.6$; $p > 0.05$), and switchgrass declined more quickly than *Miscanthus* in 2011 ($t_{180} = 3.50$; $p < 0.01$) but not in 2014 ($t_{180} = 1.02$, $p = 0.69$). When we modeled total root + rhizome biomass instead of roots alone, the slope by year interaction became significant ($F_{1,180} = 4.99$, $p < 0.05$), with the mass of all crops declining more with depth in 2014 than in 2011. With rhizome mass included there were no statistically resolvable differences in slope among perennials in either year, but the slopes of *Miscanthus* and switchgrass changed from similar to maize in 2011 (both $t_{180} < 1.9$; $p > 0.2$) to more negative than maize in 2014 (both $t_{180} > 2.9$, $p < 0.02$) because of dramatic increases in rhizome biomass near the surface.

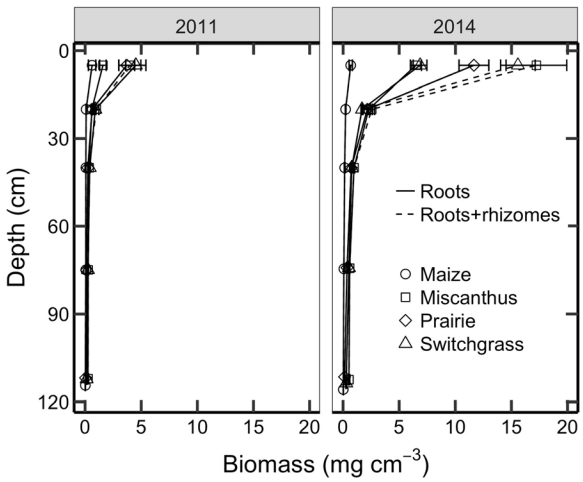

Fig. 2 Depth profiles of root and root + rhizome mass measured by deep coring in 2011 (left) and again in 2014 (right). The 2011 data are replotted from (Anderson-Teixeira et al. 2013)

Despite the observation that root biomass for maize was more evenly distributed through the soil profile (less negative slope terms) than the perennial crops, the root mass of perennials at any given depth was greater than that of maize even at the bottom of the soil profile (Fig. 1). Perennials had 2–17 times more root biomass than maize (post-hoc contrasts on fitted LS means; $t_{180} > 3$; $p < 0.01$) all the way to 128 cm, the mean maximum depth of our core samples, with the exception that in 2011 the differences between prairie and maize were marginal at depths greater than 1 m (all $t_{180} < 2.6$; all p-values $0.05 < p < 0.1$).

Minirhizotron images: Model evaluation

The Bayesian model of root distribution compensated well for poor surface root detection by the minirhizotron, explained 29% of the image-to-image variance in log root volume, and showed little bias: 90% prediction intervals for individual images included the observed value 90% of the time, and 50% intervals about 52% of the time, indicating that both the mean and variance components were consistent with the data (Fig. S3).

Much of the remaining ~70% of variation is attributable to the inherent variability among source images and could be reduced by aggregating multiple images before testing model fit, but this is prevented by the model structure. After incorporating detection and surface effects, model predictions are in units of expected *corrected* root volume and their means can no longer be compared directly against the observed means of raw images, meaning the direct comparison of observed vs. predicted values is only valid at the level of individual images. Instead, for validation of higher aggregation

levels it is more appropriate to compare model predictions against observations from coring.

Although the model predicts root *volume* per area of image rather than root mass directly, predicted root volume for midsummer 2011 and 2014 scaled positively and log-linearly against simultaneously collected root masses from coring (Fig. 3) and had similar magnitude as the values expected from a simple conversion based on previous research: If root volume per image area = (root mass)(depth of view)/(root tissue density), then the dashed lines in Fig. 3 show the root volume expected from core mass assuming 0.78 mm depth of view (Taylor et al. 2014) and root tissue densities of 0.08 g cm^{-3} for maize (Pahlavanian and Silk 1988), 0.20 for *Miscanthus* (Wahl and Ryser 2000; Roumet et al. 2006; Picon-Cochard et al. 2012), 0.19 for switchgrass (Craine et al. 2001) and 0.15 for prairie (Craine et al. 2001). With the exceptions of maize (0%) and *Miscanthus* (45%) in 2011, model predictions accounted for at least 75% of the variation in block means of root mass from cores (Fig. 3).

Qualitatively the shape of the depth function and the ranking of crop differences agreed well with the patterns seen in soil cores (Fig. 4), and did not show the reduction in near-surface root volume observed in the raw images. The model treated the variance from individual minirhizotron tubes σ^{tube} and the detection probability parameters α^{detect} and β^{detect} as identical across crops, while the intercept α, slope β, surface underdetection parameters $\alpha^{surface}$ and $\beta^{surface}$, and residual variance σ, were fit separately for each crop. Half-detection depths ($\alpha^{surface}$; the estimated depth where the surface underdetection effect reduces observations to 50% of true root volume) ranged from 7 to 33 cm in maize, 10–25 in *Miscanthus*, 14–36 in switchgrass, and 10–26 in prairie, and tended to be greatest in midseason (Fig. S2). We also attempted to fit the model with $\alpha^{surface}$ and $\beta^{surface}$ constrained to be identical across all crops, but this model failed to converge, suggesting that crop effects are important (Gelman 2008).

Minirhizotron images: Changes in root distribution through time

Across the five years of the experiment, all three perennials increased their root volume (Fig. S4, panel a; 95% intervals for difference between midsummer 2010 and 2014 root volume totals did not include 0; Fig. S4, panel

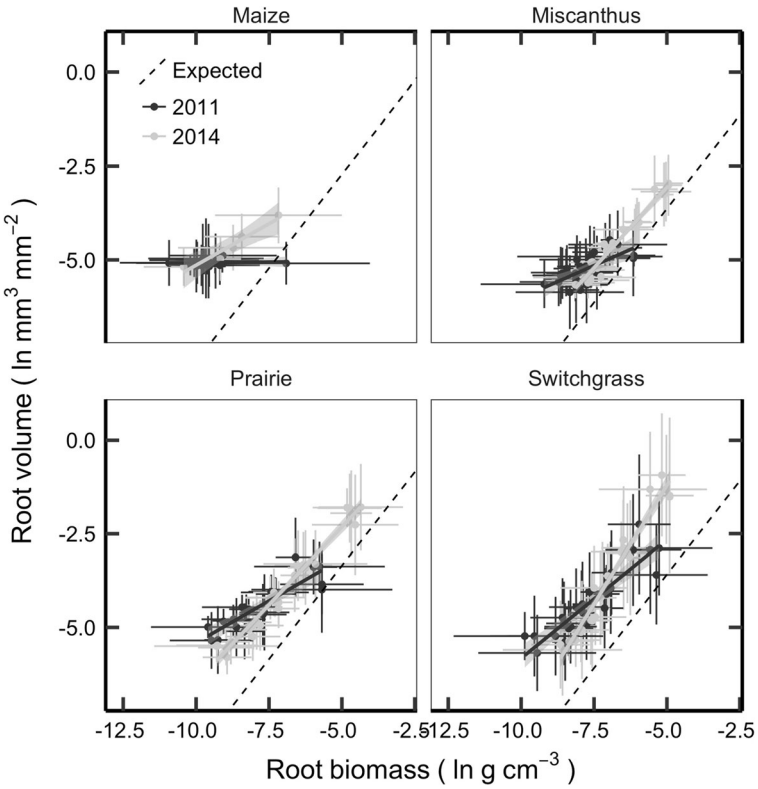

Fig. 3 Comparison between root mass measured from soil cores and root volume estimated from minirhizotron images taken in midsummer 2011 and 2014. Each point shows the mean ± 95% interval for one depth layer (0–10, 10–30, 30–50, 50–100 cm) in one experimental plot. Solid lines with shaded bands show estimate ±95% intervals for unweighted linear regressions on all plotted points in each group. Dashed lines show the expected relationship between root mass and volume assuming a 0.78 mm depth of view and constant root tissue densities of 0.08 (maize), 0.20 (*Miscanthus*), 0.19 (switchgrass), or 0.15 (prairie) g cm^{-3}

b), while maize and soybean did not (95% intervals included 0; Fig. S4, panel b). The increase in total perennial root volume came from roughly equal increases in volume at each depth (Fig. 4).

The relative distribution of root volume across depth showed little change over time (Fig. S5a). Perennial roots were slightly more concentrated near the surface in 2014 than in 2011 (slope term was more negative; 95% intervals for differences exclude 0; Fig. S5b). Maize, *Miscanthus*, and prairie all showed their most even distribution (least negative slope term) and widest uncertainty intervals in 2012, a very hot drought year, but the range of between-year differences included 0 in most cases. Only maize 2012 vs 2014 and prairie 2012 vs both 2010 and 2014 were reliably more even-rooted in 2012 than in other years (Fig. S5b). This change can be seen in the predicted depth profiles as a reduction in 2012 near-surface root volume in maize and prairie, less of a reduction in *Miscanthus*, and no visible change in switchgrass (Fig. 4).

When we followed root volume from month to month within individual growing seasons, the perennials showed strong seasonal changes in 2010 but did not change from month to month in 2012. In 2010 root volume under all four crops increased from May to August then decreased from August to October (95% intervals for differences of intercept term do not include 0; Fig. S6, panel a). The change was most marked in soybean roots, driven by a shift in slope from negative (root volume strongly decreasing with depth) in June and July to near zero (root volume near evenly distributed with depth) from midsummer through senescence (Fig. 5). In contrast, root volume in the perennial crops rose from June through August and dropped again in October, but the depth distribution did not change substantially except in *Miscanthus*, where roots were more concentrated near the surface in July than in August (Figs. 5, S6b). In 2012, maize root volume increased from May through August (Fig. S6a), but shifted its distribution dramatically from roots concentrated very near the surface in the first three observations to evenly distributed across depths in August (Fig. 6). The 2012 maize crop senesced in August because of drought and was harvested in September, so no images were collected from maize in October. All three perennials, by contrast, were consistent in total root

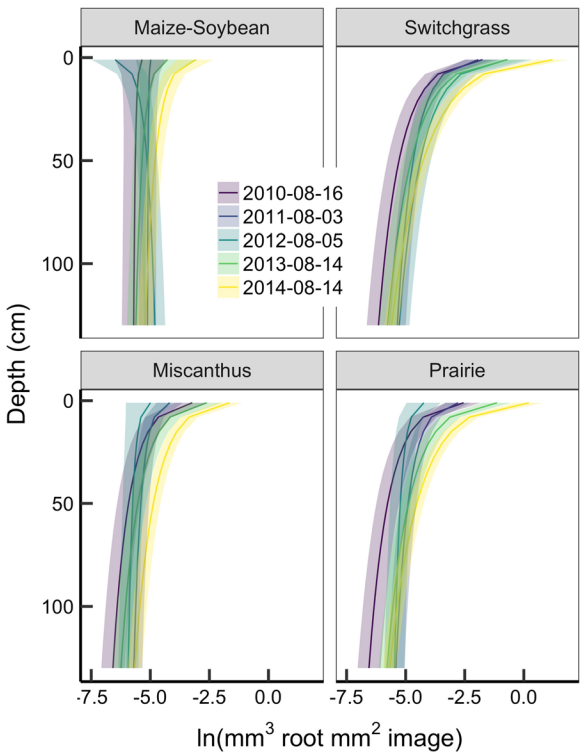

Fig. 4 Mean ± 50% intervals of estimated root volume density from minirhizotron images collected at peak aboveground biomass each year from 2010 to 2014

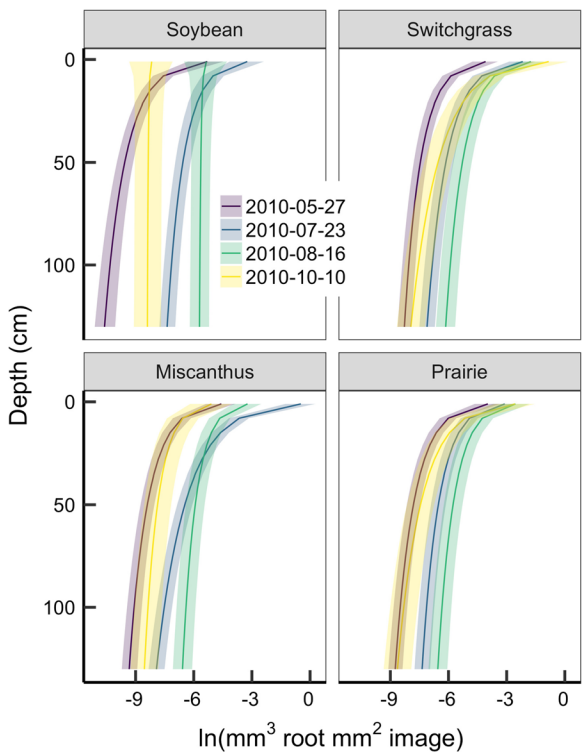

Fig. 5 Mean ± 50% intervals of estimated root volume density from minirhizotron images collected in summer 2010. Each color shows a different sampling session

volume throughout the season (95% intervals for intercept differences between sessions include 0; Fig. S6). All three perennials appeared to slightly reduce near-surface root volume late in the season (Fig. 6), but these changes were not statistically resolvable except in prairie, where roots were concentrated nearer the surface (β^{depth} more negative) in May than in either early August or October (Fig. S6b).

Discussion

In repeated observations of four crop systems, we observed more roots both by mass and by volume in perennial grasses than in annual maize-soybean. The root systems of the perennials continued to gain volume across five years of observations, were resilient to a major drought, and allocated large quantities of carbon to the deep subsoil. By explicitly correcting for depth-dependent detection biases, we found good correlation between minirhizotron and core-based measurements of root mass, and showed that the conversion factor between them can be expressed in biologically meaningful terms. With further calibration, this may allow nondestructive monitoring of root structure and C stocks in familiar units (grams instead of image areas). The combination of greatly increased root mass and allocation deep in the soil suggests that conversion from row cropping to perennial bioenergy grassess could result in substantial increases in soil C.

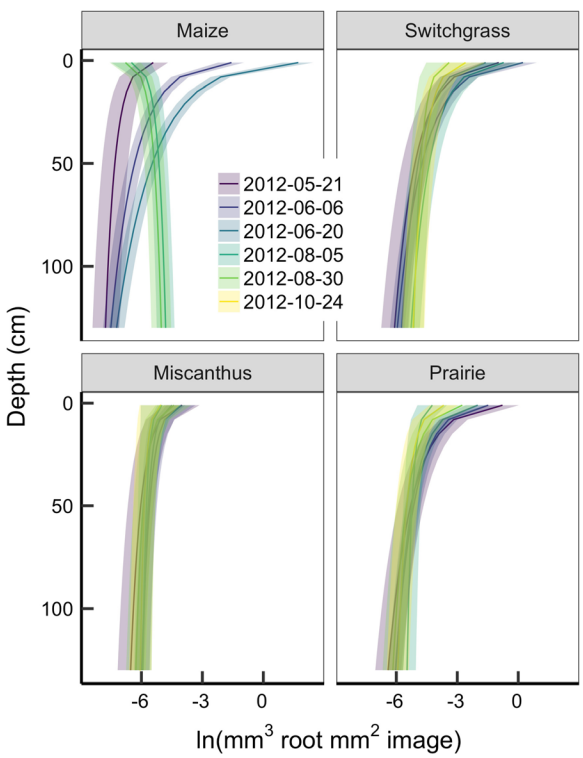

Fig. 6 Mean ± 50% intervals of estimated root volume density from minirhizotron images collected in summer 2012. Each color shows a different sampling session

Our measured root masses agree well with previous work that shows much larger root systems in perennial grasses than in annual crops, and that root mass stays high even during the spring and fall when annual fields are fallow. We observed switchgrass root masses comparable to those from other stands of similar age that were sampled to a depth of ≥90 cm (Frank et al. 2004; Monti and Zatta 2009; Collins et al. 2010; Garten et al. 2010; Dohleman et al. 2012) and higher than those sampled to shallower depths (Bransby et al. 1998). *Miscanthus* root masses were comparable but generally at the high end of totals seen in other studies (Neukirchen et al. 1999; Beuch et al. 2000; Christian et al. 2006; Monti and Zatta 2009; Amougou et al. 2011; Dohleman et al. 2012) and the values reported by other studies are highly correlated with sampling depth. *Miscanthus* rhizome mass, by contrast, was comparable but generally at the low end of totals seen in other studies, comparable to previous work on crops of similar ages (Beuch et al. 2000; Christian et al. 2006; Amougou et al. 2011; Dohleman et al. 2012). Taken together, this suggests that *Miscanthus* invested especially heavily in roots over rhizomes at our highly fertile, deep-soil site. The minirhizotron method never detected rhizomes, so all image-based results should be considered to show root volume only.

We expected that root development would approximately parallel aboveground stand development, with belowground biomass nearing steady state in year 3–4. Instead, perennials explored the whole soil profile very early in development (we detected roots beyond 126 cm even in the first imaging sessions) but their root volume continued to increase through the whole period of the study even after each crop reached maximum aboveground biomass (2010–2012; Joo et al. 2016). This increase was especially evident in the prairie treatment, which consistently had the lowest aboveground productivity among our four crop systems (Anderson-Teixeira et al. 2013) but reached 608 ± 89 g root m^{-2} by 2011 and 1924 ± 306 g root m^{-2} by 2014 (Fig. 1), making the root mass of this prairie comparable to 20-year-old

restorations in its fourth year and, remarkably, comparable in its seventh year to undisturbed native prairie remnants (Kucharik et al. 2006; Matamala et al. 2008; Jelinski et al. 2011).

During the unusually hot and dry summer of 2012, both *Miscanthus* and switchgrass maintained essentially the same root volume and depth distribution as other years, while maize and prairie shifted from shallower to deeper roots as the season progressed. This may reflect a difference in ecological drought resilience strategies, with both *Miscanthus* and switchgrass apparently able to access deep soil water and maintain growth through the drought. In fact, *Miscanthus* yields in 2012 were higher than any other year of the experiment, and switchgrass yields were comparable to those from other post-maturity years (Joo et al. 2016). Although measurements of net ecosystem exchange suggest that *Miscanthus* may have suffered some delayed consequences of 2012 drought stress in the form of reduced 2013 productivity (Joo et al. 2016), we saw no negative effects on root volume in either year. By contrast, Mann et al. (2013) reported very shallow root systems and severe biomass reductions from juvenile *Miscanthus* grown in water-limited mesocosms while juvenile switchgrass explored deep soil whether irrigated or water-limited. The difference between these results and ours may indicate that mature, established deep roots are crucial to *Miscanthus* drought resistance. If so, lack of established root systems could also explain the poor overwinter *Miscanthus* survival we observed during the first two years of the experiment. It is probable that the shift in prairie root distribution came from changes in relative dominance of species with different rooting habits rather than from individual species reallocating mass within the soil profile, but this is speculative because the minirhizotron images do not allow us to distinguish among roots of different species. Furthermore, the presence of deep roots from a particular species is not necessarily sufficient for effective access to deep soil water (Nippert et al. 2012; Hall and Sinclair 2015). Future work in mixed-species systems could resolve these ambiguities by combining minirhizotron analysis with periodic DNA analysis to determine root community composition (Mommer et al. 2008; Black 2016).

By modeling the root distribution as a log-linear function of depth and explicitly estimating two forms of detection noise (zeroes from small samples and bias from the surface underdetection effect), we gained sensitivity to detect changes in root volume that would have been invisible in a conventional minirhizotron analysis of root length density. However, this method has some limitations. It requires a large sample size (probably at least 15–20 tubes per treatment) to achieve reasonable precision, especially for the underdetection parameter estimates. In particular, estimates of the surface underdetection factor are positively correlated with model slope, so the model requires enough data from deep soil (where the underdetection factor is zero) to accurately separate these effects. In our data this was especially visible early in 2012, when few maize roots were present below the surface layers and therefore the model predicted unrealistically high maize root density in the surface layers (Fig. 6).

Previous work on the underdetection of near-surface roots by minirhizotron images has usually concluded that the underdetection is similar across species (Ephrath et al. 1999). Our model differs by estimating the correction separately for each crop; we tested an alternate model with a common correction factor but were unable to obtain model convergence, suggesting that crop-specific corrections were necessary. It is possible that this difference can be explained as a difference in time since tube installation: We re-installed the minirhizotron tubes in maize-soybean each year but left the perennial tubes in place. Consistent with this hypothesis, we note that the estimated correction factor differed more between maize-soybean and perennials than it did among perennials, but we cannot test for time effects in more detail because installation time and crop are confounded in our experimental design.

We also emphasize that our conversion from root volume to mass (Fig. 3) is based solely on mean root tissue densities from the literature; it assumes constant tissue density across depth, root age and size class, and plant development stage. This assumption was necessary because few depth- and time-resolved reports of tissue density are available. Indeed, what evidence we do have suggests variation in tissue density across all of these factors (Craine et al. 2003; Bernier et al. 2005; Monti and Zatta 2009; de Vries et al. 2016). The precision of rhizotron-based root mass estimates could likely be improved by measuring tissue density in the roots from the soil cores.

Overall we found that perennial bioenergy grasses consistently had many more roots than maize and soybean at every depth, and the deep soil layers (> 50 cm) contained more perennial roots than were present in the entire soil profile under maize or soybean. This deep rooting appears to be important for resilience to summer

drought, and our improved minirhizotron observations allow detailed quantititative monitoring of this large flux of carbon into stable, rarely disturbed soil. Consistent with previous net ecosystem exchange observations showing strong carbon uptake by perennial crops compared to losses from maize-soybean rotation (Zeri et al. 2011), we therefore expect that the conversion from row crops to perennial bioenergy grasses will result in large and persistent increases in soil C storage.

Acknowledgements We are grateful to R. J. Cody Markelz, John Brehm, and Laurel Brehm for statistical advice, and to Abisheik Pal, Christopher Sligar, Edwin Albrarran, Jacob Rosenthal, Michael Donovan, and Taylor Wright for their endless patience performing the root tracing. This research was funded by the Energy Biosciences Institute. The authors declare that they have no conflict of interest.

References

Agostini F, Gregory AS, Richter GM (2015) Carbon sequestration by perennial energy crops: is the jury still out? Bioenergy Res 8:1057–1080. doi:10.1007/s12155-014-9571-0

Amougou N, Bertrand I, Machet J-M, Recous S (2011) Quality and decomposition in soil of rhizome, root and senescent leaf from *Miscanthus x giganteus*, as affected by harvest date and N fertilization. Plant Soil 338:83–97. doi:10.1007/s11104-010-0443-x

Anderson-Teixeira KJ, Masters MD, Black CK et al (2013) Altered belowground carbon cycling following land-use change to perennial bioenergy crops. Ecosystems 16:508–520. doi:10.1007/s10021-012-9628-x

Balesdent J, Balabane M (1996) Major contribution of roots to soil carbon storage inferred from maize cultivated soils. Soil Biol Biochem 28:1261–1263. doi:10.1016/0038-0717(96)00112-5

Bardgett RD, Mommer L, De Vries FT (2014) Going underground: root traits as drivers of ecosystem processes. Trends Ecol Evol 29:692–699. doi:10.1016/j.tree.2014.10.006

Bernier PY, Robitaille G, Rioux D (2005) Estimating the mass density of fine roots of trees for minirhizotron-based estimates of productivity. Can J For Res 35:1708–1713. doi:10.1139/x05-099

Beuch S, Boelcke B, Belau L (2000) Effect of the organic residues of *Miscanthus* × *giganteus* on the soil organic matter level of arable soils. J Agron Crop Sci 183:111–119. doi:10.1046/j.1439-037x.2000.00367.x

Black CK (2016) Plant root contributions to the carbon balance of a changing agricultural Midwest. University of Illinois Urbana-Champaign, USA, Doctoral Dissertation, p 131

Black CK, Masters MD, LeBauer DS et al (2017) Data from: root volume distribution of maturing perennial grasses revealed by correcting for minirhizotron surface effects. doi:10.5061/dryad.79822. Accessed 27 Jun 2017

Bohm W, Maduakor H, Taylor HM (1977) Comparison of five methods for characterizing soybean rooting density and development. Agron J 69:415–419. doi:10.2134/agronj1977.00021962006900030021x

Bragg PL, Govi G, Cannell RQ (1983) A comparison of methods, including angled and vertical minirhizotrons, for studying root growth and distribution in a spring oat crop. Plant Soil 73:435–440. doi:10.1007/BF02184322

Bransby DI, McLaughlin SB, Parrish DJ (1998) A review of carbon and nitrogen balances in switchgrass grown for energy. Biomass Bioenergy 14:379–384. doi:10.1016/S0961-9534(97)10074-5

Carpenter B, Gelman A, Hoffman MD et al (2017) Stan: a probabilistic programming language. J Stat Softw 76:1–32. doi:10.18637/jss.v076.i01

Christian DG, Poulton PR, Riche AB et al (2006) The recovery over several seasons of ^{15}N-labelled fertilizer applied to *Miscanthus* × *giganteus* ranging from 1 to 3 years old. Biomass Bioenergy 30:125–133. doi:10.1016/j.biombioe.2005.11.002

Collins HP, Smith JL, Fransen S et al (2010) Carbon sequestration under irrigated switchgrass (*Panicum virgatum* L.) production. Soil Sci Soc Am J 74:2049–2058. doi:10.2136/sssaj2010.0020

Comas LH, Eissenstat DM (2009) Patterns in root trait variation among 25 co-existing north American forest species. New Phytol 182:919–928. doi:10.1111/j.1469-8137.2009.02799.x

Craine JM, Froehle J, Tilman DG et al (2001) The relationships among root and leaf traits of 76 grassland species and relative abundance along fertility and disturbance gradients. Oikos 93:274–285. doi:10.1034/j.1600-0706.2001.930210.x

Craine JM, Wedin DA, Chapin FS III, Reich PB (2003) The dependence of root system properties on root system biomass of 10 north American grassland species. Plant Soil 250:39–47. doi:10.1023/A:1022817813024

De Deyn GB, Cornelissen JHC, Bardgett RD (2008) Plant functional traits and soil carbon sequestration in contrasting biomes. Ecol Lett 11:516–531. doi:10.1111/j.1461-0248.2008.01164.x

de Vries FT, Brown C, Stevens CJ (2016) Grassland species root response to drought: consequences for soil carbon and nitrogen availability. Plant Soil. doi:10.1007/s11104-016-2964-4

Dohleman FG, Heaton EA, Arundale RA, Long SP (2012) Seasonal dynamics of above- and below-ground biomass and nitrogen partitioning in *Miscanthus* × *giganteus* and *Panicum virgatum* across three growing seasons. Glob Chang Biol Bioenergy 4:534–544. doi:10.1111/j.1757-1707.2011.01153.x

Ephrath JE, Silberbush M, Berliner P (1999) Calibration of minirhizotron readings against root length density data obtained from soil cores. Plant Soil 209:201–208. doi:10.1023/A:1004556100253

Frank AB, Berdahl JD, Hanson JD et al (2004) Biomass and carbon partitioning in switchgrass. Crop Sci 44:1391–1396. doi:10.2135/cropsci2004.1391

Garten CT Jr, Smith JL, Tyler DD et al (2010) Intra-annual changes in biomass, carbon, and nitrogen dynamics at 4-year old switchgrass field trials in west Tennessee, USA. Agric Ecosyst Environ 136:177–184. doi:10.1016/j.agee.2009.12.019

Gelman A (2006) Prior distributions for variance parameters in hierarchical models (comment on article by Browne and Draper). Bayesian Anal 1:515–534. doi:10.1214/06-BA117A

Gelman A (2008) The folk theorem of statistical computing http://andrewgelman.com/2008/05/13/the_folk_theore/. Accessed 2 Dec 2016

Gelman A, Rubin DB (1992) Inference from iterative simulation using multiple sequences. Stat Sci 7:457–472. doi:10.1214/ss/1177011136

Genney DR, Alexander IJ, Hartley SE (2002) Soil organic matter distribution and below-ground competition between *Calluna vulgaris* and *Nardus stricta*. Funct Ecol 16:664–670. doi:10.1046/j.1365-2435.2002.00667.x

Gray SB, Dermody O, Klein SP et al (2016) Intensifying drought eliminates the expected benefits of elevated carbon dioxide for soybean. Nat Plants 2:16132. doi:10.1038/nplants.2016.132

Hall AJ, Sinclair TR (2015) Rooting front and water uptake: what you see and get may differ. Agron J 107:1766. doi:10.2134/agronj14.0551

Hodge A (2004) The plastic plant: root responses to heterogeneous supplies of nutrients. New Phytol 162:9–24. doi:10.1111/j.1469-8137.2004.01015.x

Iversen CM, Murphy MT, Allen MF et al (2011) Advancing the use of minirhizotrons in wetlands. Plant Soil 352:23–39. doi:10.1007/s11104-011-0953-1

Jelinski NA, Kucharik CJ, Zedler JB (2011) A test of diversity-productivity models in natural, degraded, and restored wet prairies. Restor Ecol 19:186–193. doi:10.1111/j.1526-100X.2009.00551.x

Johnson MG, Tingey DT, Phillips DL, Storm MJ (2001) Advancing fine root research with minirhizotrons. Environ Exp Bot 45:263–289. doi:10.1016/S0098-8472(01)00077-6

Joo E, Hussain MZ, Zeri M et al (2016) The influence of drought and heat stress on long-term carbon fluxes of bioenergy crops grown in the Midwestern USA. Plant Cell Environ 39:1928–1940. doi:10.1111/pce.12751

Kell DB (2011) Breeding crop plants with deep roots: their role in sustainable carbon, nutrient and water sequestration. Ann Bot 108:407–418. doi:10.1093/aob/mcr175

Kochian LV (2016) Root architecture. J Integr Plant Biol 58:190–192. doi:10.1111/jipb.12471

Kucharik CJ, Fayram NJ, Cahill KN (2006) A paired study of prairie carbon stocks, fluxes, and phenology: comparing the world's oldest prairie restoration with an adjacent remnant. Glob Chang Biol 12:122–139. doi:10.1111/j.1365-2486.2005.01053.x

Lenth RV (2016) Least-squares means: the R package lsmeans. J Stat Softw 69:1–33. doi:10.18637/jss.v069.i01

Liu B, Li H, Zhu B et al (2015) Complementarity in nutrient foraging strategies of absorptive fine roots and arbuscular mycorrhizal fungi across 14 coexisting subtropical tree species. New Phytol 208:125–136. doi:10.1111/nph.13434

Lynch JP, Brown KM (2001) Topsoil foraging – an architectural adaptation of plants to low phosphorus availability. Plant Soil 237:225–237. doi:10.1023/A:1013324727040

Mann JJ, Barney JN, Kyser GB, DiTomaso JM (2013) Root system dynamics of *Miscanthus* × *giganteus* and *Panicum virgatum* in response to rainfed and irrigated conditions in California. Bioenergy Res 6:678–687. doi:10.1007/s12155-012-9287-y

Masters MD, Black CK, Kantola IB et al (2016) Soil nutrient removal by four potential bioenergy crops: *Zea mays*, *Panicum virgatum*, *Miscanthus* × *giganteus*, and prairie. Agric Ecosyst Environ 216:51–60. doi:10.1016/j.agee.2015.09.016

Matamala RR, Jastrow JD, Miller RM, Garten CT (2008) Temporal changes in C and N stocks of restored prairie: implications for C sequestration strategies. Ecol Appl 18:1470–1488. doi:10.1890/07-1609.1

McCalmont JP, Hastings A, McNamara NP et al (2015) Environmental costs and benefits of growing *Miscanthus* for bioenergy in the UK. Glob Chang Biol Bioenergy. doi:10.1111/gcbb.12294

Metcalfe DB, Meir P, Williams M (2007) A comparison of methods for converting rhizotron root length measurements into estimates of root mass production per unit ground area. Plant Soil 301:279–288. doi:10.1007/s11104-007-9447-6

Milchunas DG (2009) Estimating root production: comparison of 11 methods in shortgrass steppe and review of biases. Ecosystems 12:1381–1402. doi:10.1007/s10021-009-9295-8

Mokany K, Raison RJ, Prokushkin AS (2006) Critical analysis of root : shoot ratios in terrestrial biomes. Glob Chang Biol 12:84–96. doi:10.1111/j.1365-2486.2005.001043.x

Mommer L, Wagemaker CAM, de Kroon H, Ouborg NJ (2008) Unravelling below-ground plant distributions: a real-time polymerase chain reaction method for quantifying species proportions in mixed root samples. Mol Ecol Resour 8:947–953. doi:10.1111/j.1755-0998.2008.02130.x

Monti A, Zatta A (2009) Root distribution and soil moisture retrieval in perennial and annual energy crops in northern Italy. Agric Ecosyst Environ 132:252–259. doi:10.1016/j.agee.2009.04.007

Neukirchen D, Himken M, Lammel J et al (1999) Spatial and temporal distribution of the root system and root nutrient content of an established *Miscanthus* crop. Eur J Agron 11:301–309. doi:10.1016/S1161-0301(99)00031-3

Nippert J, Wieme R, Ocheltree T, Craine JM (2012) Root characteristics of C_4 grasses limit reliance on deep soil water in tallgrass prairie. Plant Soil 355:385–394. doi:10.1007/s11104-011-1112-4

Pahlavanian AM, Silk WK (1988) Effect of temperature on spatial and temporal aspects of growth in the primary maize root. Plant Physiol 87:529–532. doi:10.1104/pp.87.2.529

Parker CJ, Carr MKV, Jarvis NJ et al (1991) An evaluation of the minirhizotron technique for estimating root distribution in potatoes. J Agric Sci 116:341–350. doi:10.1017/S0021859600078151

Picon-Cochard C, Pilon R, Tarroux E et al (2012) Effect of species, root branching order and season on the root traits of 13 perennial grass species. Plant Soil 353:47–57. doi:10.1007/s11104-011-1007-4

Pierret A, Moran CJ, Doussan C (2005) Conventional detection methodology is limiting our ability to understand the roles and functions of fine roots. New Phytol 166:967–980. doi:10.1111/j.1469-8137.2005.01389.x

Pinheiro J, Bates D, DebRoy S et al (2016) Nlme: linear and nonlinear mixed effects models. R package version 3.1–128. http://CRAN.R-project.org/package=nlme. Accessed 21 Jun 2016

Poorter H, Bühler J, van Dusschoten D et al (2012) Pot size matters: a meta-analysis of the effects of rooting volume on plant growth. Funct Plant Biol 39:839–850. doi:10.1071/FP12049

Prieto I, Stokes A, Roumet C (2016) Root functional parameters predict fine root decomposability at the community level. J Ecol 104:725–733. doi:10.1111/1365-2745.12537

R Core Team (2016) R: A language and environment for statistical computing Version 3.3.2. https://www.R-project.org/. Accessed 19 Jan 2017

Rasse DP, Rumpel C, Dignac M-F (2005) Is soil carbon mostly root carbon? Mechanisms for a specific stabilisation. Plant Soil 269:341–356. doi:10.1007/s11104-004-0907-y

Roberts MJ, Long SP, Tieszen LL, Beadle CL (1993) Measurement of plant biomass and net primary production of herbaceous vegetation. In: Hall DO, Scurlock JMO, Bolhar-Nordenkampf HR et al (eds) Photosynthesis and production in a changing environment: a field and laboratory manual. Chapman Hall, New York, pp 1–21

Rose L (2017) Pitfalls in root trait calculations: how ignoring diameter heterogeneity can lead to overestimation of functional traits. Front Plant Sci 8:898. doi:10.3389/fpls.2017.00898

Roumet C, Urcelay C, Díaz S (2006) Suites of root traits differ between annual and perennial species growing in the field. New Phytol 170:357–368. doi:10.1111/j.1469-8137.2006.01667.x

Rumpel C, Kögel-Knabner I (2011) Deep soil organic matter—a key but poorly understood component of terrestrial C cycle. Plant Soil 338:143–158. doi:10.1007/s11104-010-0391-5

Samson BK, Sinclair TR (1994) Soil core and minirhizotron comparison for the determination of root length density. Plant Soil 161:225–232. doi:10.1007/BF00046393

Smith CM, David MB, Mitchell CA et al (2013) Reduced nitrogen losses after conversion of row crop agriculture to perennial biofuel crops. J Environ Qual 42:219–228. doi:10.2134/jeq2012.0210

Sonderegger DL, Ogle K, Evans RD et al (2013) Temporal dynamics of fine roots under long-term exposure to elevated CO_2 in the Mojave Desert. New Phytol 198:127–138. doi:10.1111/nph.12128

Stan Development Team (2016a) RStan: the R interface to Stan. R package version 2.14.1. https://cran.r-project.org/web/packages/rstan/. Accessed 19 Jan 2017

Stan Development Team (2016b) Stan Modeling Language Users Guide and Reference Manual, version 2.14.0. http://mc-stan.org. Accessed 19 Jan 2017

Taylor HM, Upchurch D, McMichael B (1990) Application and limitation of rhizotrons and minirhizotrons for root studies. Plant Soil 129:29–35. doi:10.1007/BF00011688

Taylor BN, Beidler KV, Strand AE, Pritchard SG (2014) Improved scaling of minirhizotron data using an empirically-derived depth of field and correcting for the underestimation of root diameters. Plant Soil 374:941–948. doi:10.1007/s11104-013-1930-7

Topp CN, Bray AL, Ellis NA, Liu Z (2016) How can we harness quantitative genetic variation in crop root systems for agricultural improvement? J Integr Plant Biol 58:213–225. doi:10.1111/jipb.12470

Wahl S, Ryser P (2000) Root tissue structure is linked to ecological strategies of grasses. New Phytol 148:459–471. doi:10.1046/j.1469-8137.2000.00775.x

Ward SE, Smart SM, Quirk H et al (2016) Legacy effects of grassland management on soil carbon to depth. Glob Chang Biol 22:2829–2938. doi:10.1111/gcb.13246

Wasson AP, Richards RA, Chatrath R et al (2012) Traits and selection strategies to improve root systems and water uptake in water-limited wheat crops. J Exp Bot 63:3485–3498. doi:10.1093/jxb/ers111

Zeri M, Anderson-Teixeira KJ, Hickman GC et al (2011) Carbon exchange by establishing biofuel crops in Central Illinois. Agric Ecosyst Environ 144:319–329. doi:10.1016/j.agee.2011.09.006

Zwicke M, Picon-Cochard C, Morvan-Bertrand A et al (2015) What functional strategies drive drought survival and recovery of perennial species from upland grassland? Ann Bot 116:1001–1015. doi:10.1093/aob/mcv037